Journal of the Korean Ceramic Society
Vol. 38, No. 10, pp. 881~885, 2001.

Formation Mechanism of Intermediate Phase in $Ba(Mg_{1/3}Ta_{2/3})O_3$ Microwave Dielectrics

Yonghan Fang* and Young-Jei Oh†

Materials Science & Technology Division, Cheongryang, Korea Institute of Science and Technology, Seoul 136-791, Korea
**Department of Inorganic Materials, Shanghai University, Jiading, Shanghai 201800, China*
(Received September 15, 2001; Accepted October 10, 2001)

ABSTRACT

Kinetics and mechanisms of intermediate phases formation in $Ba(Mg_{1/3}Ta_{2/3})O_3$, obtained by a solid state reaction were studied. $BaTa_2O_6$ and $Ba_4Ta_2O_9$ as intermediate products were first formed at 700°C. $Ba(Mg_{1/3}Ta_{2/3})O_3$ was appeared at 800°C. Several reactions take place on heating process. $BaTa_2O_6$ is found at the first stage of the reaction, and then $BaTa_2O_6$ or $Ba_4Ta_2O_9$ react with MgO to form $Ba(Mg_{1/3}Ta_{2/3})O_3$. The reaction of $Ba(Mg_{1/3}Ta_{2/3})O_3$ formation does not complete until fired at 1350°C for 60 min. The kinetics of solid-state reaction between powdered reactants was controlled by diffusion mechanism, and can be explained by the Jander's model for three-dimensional diffusion.

Key words : $Ba(Mg_{1/3}Ta_{2/3})O_3$, $BaTa_2O_6$, $Ba_4Ta_2O_9$, Intermediate phase, Kinetics, Diffusion mechanism, Jander's model

1. Introduction

$Ba(Mg_{1/3}Ta_{2/3})O_3$ (herein designated as BMT) is one of the few complex perovskite compounds that exhibits ultra-low dielectric loss at microwave frequencies (>10 GHz). Its quality factor ($Q \cdot f$) was reported the range of 150,000 to 360,000 GHz, dielectric constant of 25 and almost zero temperature coefficient of frequency.[1-5] These distinguishing features of BMT have resulted in considerable interest on the synthesis of this material.[4,6-11] However, the problem is that BMT ceramic is difficult to sinter. In general, the sintering temperature of BMT ceramics is higher than 1600°C. Many works on this material have been performed in order to improve the sinterability. Solution chemistry technique offers an alternative approach for synthesis of BMT powders.[6-9] Dense mono-phase BMT ceramics (96%-98% of the theoretical density) were prepared at low firing temperature of 1400°C using the sol-gel derived powder.[6] However the $Q \cdot f$ product of the BMT ceramics prepared by solution chemistry technique was lower than that of the conventional solid-state reaction method.[6,7] Therefore it becomes important to analyze the phase development and formation mechanism according to firing process in solid state reaction.

Furthermore, there is little information concerning the mechanism and kinetics of the BMT formation by solid-state reaction in literature. Kakeqawa et al. found that only $BaTa_2O_6$ was formed as an intermediate product by the solid-state reaction method.[7]

The first theoretical model for the mechanism and kinetics of solid-state reaction on the powdered reactants had formulated by Jander in 1927.[12,13] Since then, a large number of rate equations (models) have been proposed. The rates of reactions are usually interpreted in terms of various equations based on physical models, but not always with great success. In addition, the rate of solid-state reaction depends on the factors of particle size, its distribution and previous history of the reactants themselves. So, in this study the particle system with narrow size distribution (≈ 1 to 3 μm) was selected. To clarify the mechanisms and kinetics of the BMT formation, we investigated the system of $BaCO_3 \cdot 1/3\ MgO \cdot 1/3\ Ta_2O_5$ using isothermal quenching technique, thermal analysis and X-ray diffractometry.

2. Experimental

Barium carbonate (99.9%), magnesium oxide (99.9%) and tantalum oxide (99.95%) were used as raw materials. The molar ratio of $BaCO_3$: MgO: Ta_2O_5 was 1: 1/3: 1/3. The samples were prepared by grinding the oxides mixture in a milling pot containing agate balls and distilled water. The particle size of the mixture was reduced to ≈ 1 to 3 μm after grinding. The mixture was then dried at 100°C for 4 h.

The samples in a small platinum crucible were placed at hot zone of the tube furnace being controlled within ± 1°C. Two sets of experiments were carried out. The first set was designed to investigate the sequence of phase change of the mixtures during heating. The phase changes in this mixture are plotted in Fig. 1 as a function of firing temperature. The samples in this set were heated up to the desired temperature with heating rate of 600°C/h, and then air quenched. The weight of the sample was also measured before and after quenching, respectively, to know the weight loss of

†Corresponding author : youngjei@kist.re.kr

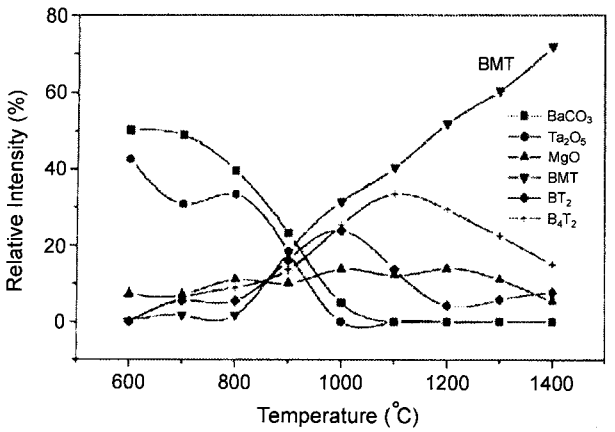

Fig. 1. Phases intensity (%) vs. reaction temperature for BMT samples with heating rate of 600°C/h.

each sample.

The second set of the experiments was designed to study the kinetics. The samples were treated at selected temperatures for up to 720 min. and air took out from the furnace with intervals of 5, 15, 30, 60, 120, 180, 240, 720 min, and then air quenched.

When barium carbonate reacts with other reactants, the weight of sample will be reduced corresponding to the reaction. So the weight loss variation of the samples could be used as a measurement tool for the extent of reaction. An extent of reaction, a, is defined as the ratio of the measured weight loss to the total weight loss. Phase analysis of the quenched samples was performed by X-ray diffractometery (CuKα, λ = 0.154056 nm). The powders were scanned between 10° and 75° at 2θ-ω scanning mode. Silicon powder was used as a calibration standard to calibrate the data.

3. Results and Discussion

3.1. Intermediate phase and BMT formation mechanism

In order to trace the reaction of BMT formation, the mixtures were heated and quenched at various temperatures without soaking time. Intermediate phases of $BaTa_2O_6$ and $Ba_4Ta_2O_9$ were formed at 700°C as shown in Fig. 1. When the temperature was raised above 800°C, however, $BaTa_2O_6$ and $Ba_4Ta_2O_9$ begun to react with MgO to form the BMT, simultaneously with the further formation of $BaTa_2O_6$ and $Ba_4Ta_2O_9$. At temperatures above 1000° and 1100°C, $BaTa_2O_6$ and $Ba_4Ta_2O_9$ begun to disappear respectively. The amount of BMT was linearly increased with increment of heating temperature. However, two intermediate products, $BaTa_2O_6$ and $Ba_4Ta_2O_9$, were presented until 1400 °C. Fig. 1 clearly shows that the following reactions took place during heating:

$$BaCO_3 + Ta_2O_5 \rightarrow BaTa_2O_6 + CO_2 \uparrow \quad (1)$$

$$BaTa_2O_6 + 3\ BaCO_3 \rightarrow Ba_4Ta_2O_9 + 3\ CO_2 \uparrow \quad (2)$$

$$Ba_4Ta_2O_9 + 1/3MgO \rightarrow Ba(Mg_{1/3}Ta_{2/3})O_3 + 2/3\ BaTa_2O_6 + 7/3\ BaO \quad (3)$$

$$BaTa_2O_6 + 1/3MgO \rightarrow Ba(Mg_{1/3}Ta_{2/3})O_3 + 1/3\ Ta_2O_5 \quad (4)$$

$$BaO + Ta_2O_5 \rightarrow BaTa_2O_6 \quad (5)$$

Both reactions (1) and (2) start at 700°C and the rate of these reactions is very fast, while both (3) to (5) start at 800°C. At the temperature range between 800°C to 1000°C, three reactions of -(1), (2) and (3)-are preceeded simultaneously. When the temperature is over 1000°C, the reactions are followed by the processes (3), (4) and (5). According to reactions (3) to (5), the formation of one mole BMT is accompanied by the appearance of equivalent amount of Ta_2O_5 or $BaTa_2O_6$. This may be the reason of secondary phases observation at such a high temperatures. Intermediate products of reations (3)–(5) can exist also up to 1400°C.

According to the reactions (1) and (2), the fractions reacted can be measured by weight change during heating. The mixtures of starting materials were heated at 700°, 800°, 900° and 1000°C, respectively for desired soaking time and then quenched. The weight losses of the samples before and after quenching were measured. Fig. 2 shows fraction transformed (α) at various reaction temperatures and times. All curves except at 700°C show a typical parabola. This parabolic curve means the characteristics of diffusion-controlled reaction.

3.2. Kinetics

Theoretical kinetic equations have been derived over the past 60 years for solid-state reactions of powder. Basically, solid state reactions can be explained by (a) diffusion-controlled reactions, (b) mechanisms controlled by nucleation and growth of the product, or (c) processes occurring at interfaces, i.e. phase boundary-controlled reactions and kinetic equations based on the order of reaction.

The rate equations tested in this experiment are shown in Table 1. To identify the rate equation, the fraction transformed, α vs. time is usually examined by linear plotting F (α) vs. time. In this investigation the results were compared by graphical analysis. The results from weight change shown in Fig. 2 and Table 2 were analyzed whether coincided with the various equations in Table 1. Criterion for "good fit" is that result should exhibit a linear or preferably proportional relation throughout the whole experimental range. The results suggest that only diffusion equation is satisfying to describe the reaction, as their plots of F (α) vs. time. The final results fit with D3, D4 and D5 models well, but is almost equal to Jander's equation (6):

$$[1 - (1 - \alpha)^{1/3}]^2 = kt \quad (6)$$

where α is fraction transformed, k constant of reaction rate and t time. Fig. 3 shows the plots of F (α) vs time as a function of heating temperature. This Jander's equation explains the kinetic reactions satisfactorily, and follows the curve describing the diffusion-controlled mechanism. The

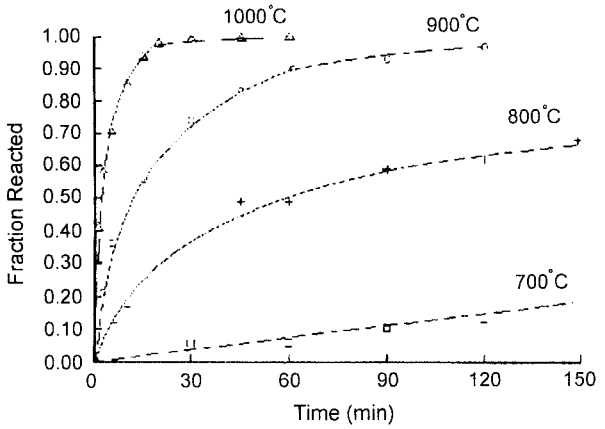

Fig. 2. Fraction reacted, a vs. soaking time at various temperature for the reaction: $4BaCO_3 + Ta_2O_5 \rightarrow Ba_4Ta_2O_9 + CO_2\uparrow$.

Table I. Equation Summary of Process Types

Symbols	Model (Type of process)	Equations	
		y	x
ϕ	Zero order (Beretka)	α	t
D1	One-dimension diffusion (Beretka)	α^2	t
D2	Two-dimension diffusion (Beretka)	$(1-\alpha)\ln(1+\alpha)+\alpha$	t
D3	Diffusion (Jander)	$[1-(1-\alpha)^{1/3}]^2$	t
D4	Diffusion (Ginstling and Brounshtein)	$(1-2\alpha/3)-(1-\alpha)^{2/3}$	t
D5	Diffusion (Carter)	$(1+\alpha)2/3+(1-\alpha)^{2/3}$	t
F1	First-order kinetics (empirical)	$-\ln(1+\alpha)^{1/2}$	t
R2	Phase boundary (disk)	$1-(1+\alpha)^{1/3}$	t
R3	Phase boundary (sphere)	$1-(1-\alpha)^{1/3}$	t
A2	Nucleation (Avrami)	$[-\ln(1+\alpha)]^{1/2}$	t

data also shows that reactions (1) and (2) will be finished at 1000°C for about 30 min as shown in Table 2. This result is also confirmed by X-ray diffraction analysis. $BaCO_3$ was not found in the sample fired at 1000°C for 30 min.

The samples heated at the temperature range from 600°C to 1350°C for 60 min were analyzed by X-ray quantitatively as shown in Fig. 4. $Ba_4Ta_2O_9$ phase was found at 700°C and BMT phase was found at 800°C. At 1000°C reactants $BaCO_3$ and Ta_2O_5 disappear but MgO still appear until 1250°C. Further experiments show that second phase $Ba_4Ta_2O_9$ is also present in the sample heated at 1350°C for 60 min. Fig. 5 plots the relative intensity of phases as a function of firing temperature with 60 min soaking time. BMT and second phase, $Ba_4Ta_2O_9$, were found at 800°C. No $BaTa_2O_6$ was found in this set of samples. It implies that the rate of reaction (2) of $Ba_4Ta_2O_9$ formation is much higher than that of reaction (1) so that no $BaTa_2O_6$ can be detected. $Ba_4Ta_2O_9$ was increased with increment of firing temperature until

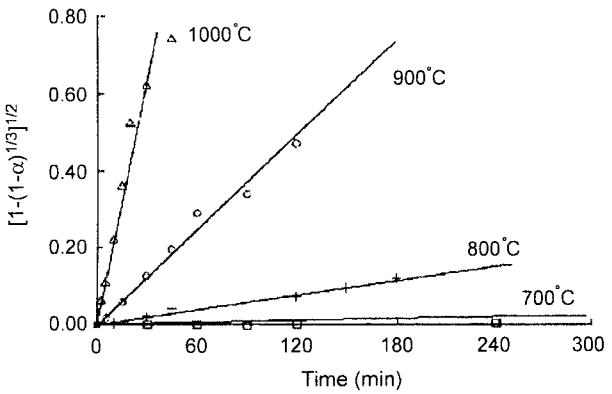

Fig. 3. Change in fraction reacted at different temperatures fit to Jander's equation for the reaction: $4BaCO_3 + Ta_2O_5 \rightarrow Ba_4Ta_2O_9 + CO_2\uparrow$.

Table 2. Fraction of Reaction Product Formed at Various Heat Conditions

700°C		800°C		900°C		1000°C	
t (min)	α	t (min)	α	t (min)	α	t (min)	α
0	0.00	0	0.00	0	0.00	0.0	0.00
30	0.0576	6	0.12	2.5	0.21	1.0	0.410
60	0.0598	10	0.17	5.0	0.36	2.5	0.579
90	0.1042	30	0.37	15.0	0.56	5.0	0.708
120	0.1334	45	0.49	30.0	0.74	10.0	0.853
240	0.1779	60	0.49	45.0	0.83	15.0	0.936
720	0.4499	90	0.59	61.0	0.90	20.0	0.979
		120	0.62	90.0	0.93	30.0	0.991
		150	0.68	120.0	0.97	45.0	0.997
		180	0.73	180.0	1.00	60.0	1.000
		210	0.72			90.0	0.994

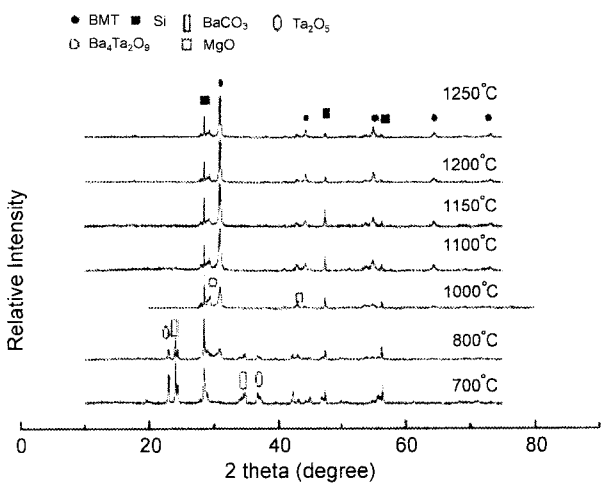

Fig. 4. XRD patterns for BMT samples heated at various temperatures for 60 min.

1000°C. The rate of BMT formation mainly depends on the rate of reaction (3). BMT was increased with increasing

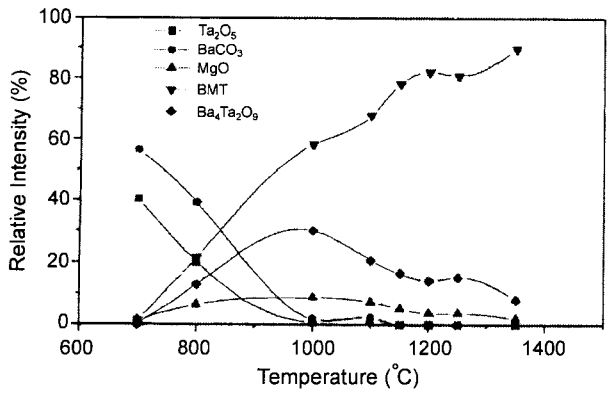

Fig. 5. Relative intensity (%) vs. heat temperature for the samples with various temperatures for 60 min.

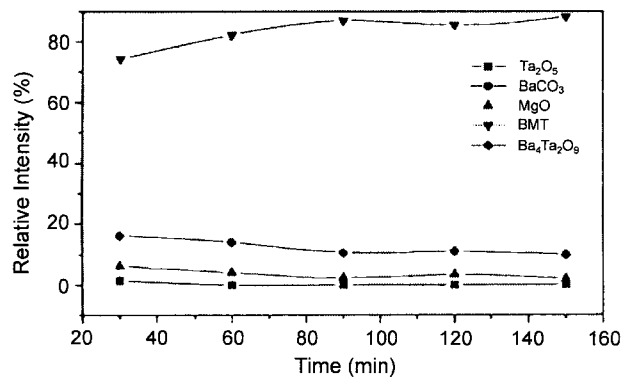

Fig. 6. Relative intensity (%) of phase vs. soaking time for the samples heated at 1200°C.

temperature linearly until 1350°C. However, MgO and $Ba_4Ta_2O_9$ were still presented as second phases even at 1350°C.

Fig. 6. shows the relative amount of phases for the samples heated at 1200°C with various soaking times. The intensity of BMT increases clearly before 60 min soaking, but the intensity increases slowly after that. It implies that even extended soaking time at 1200°C is not enough to finish the reaction.

3.3. Interpretation of reaction path

Two intermediate phases are possible to react with MgO to form the BMT. One path is that $BaTa_2O_6$ is produced by equation (1) and then quickly reacted with $BaCO_3$ to produce $Ba_4Ta_2O_9$ by reaction (2). Finally $Ba_4Ta_2O_9$ further reacts with MgO and O_2 by reaction (3) to form BMT. There are three consecutive steps in this first process. This path is called $Ba_4Ta_2O_9$ path (path I). The other path: $BaTa_2O_6$ is produced by equation (1), and then reacted with MgO to form BMT directly by reaction (4). There are two consecutive steps in this second process, which is called $BaTa_2O_6$ path (path II). Therefore, two possible parallel paths for BMT formation are considered. From the data shown in Figs. 4, 5 and 6, only $Ba_4Ta_2O_9$ was found in this experiment set. Therefore, the $Ba_4Ta_2O_9$ path is the major contributor in the overall processes, while $BaTa_2O_6$ path with much higher energy barrier is less important. The path I with the lowest energy barrier should be the most rapid and thus the major contributor to the overall process.

The overall rate of complex process is involving a series of consecutive steps. The rate of the slowest individual step seems to be step 3 in the path I process. Therefore, the rate of BMT formation would be controlled by the reaction (3). There are three steps in the path I for BMT formation, but the rates of these individual reactions is different. Therefore, the kinetics of BMT formation needs to be described step by step. In this study we only describe the kinetics of the first step in the process. The kinetics of BMT formation by reaction (3) is not explained due to the lack of data for this reaction.

4. Conclusion

$BaTa_2O_6$ and $Ba_4Ta_2O_9$ as intermediate phase are first produced at 700°C, then $Ba(Mg_{1/3}Ta_{2/3})O_3$ is appeared at 800°C. $BaTa_2O_6$ is found at the first stage of the reaction, and then $BaTa_2O_6$ or $Ba_4Ta_2O_9$ react with MgO to form $Ba(Mg_{1/3}Ta_{2/3})\ O_3$. The second phase, $Ba_4Ta_2O_9$, is presented even at 1350°C. However $BaTa_2O_6$ phase is not found at 700 °C 60 min soaking. The path I with the lowest energy barrier should be the most rapid and the major contributor to the overall process. The kinetics of solid-state reaction between reactants is controlled by diffusion mechanism, and can be explained by the Jander's model.

REFERENCES

1. S. Nomura, K. Toyama and K. Kaneta, "$Ba(Mg_{1/3}Ta_{2/3})O_3$ Ceramics with Temperature-stable High Dielectric Constant and Low Microwave Loss," *Jpn. J. Appl. Phys.*, **21** (10), L624- L626 (1982).
2. K. Matsumoto, T. Hiuga, K. Takada and H. Ichimura, "$Ba(Mg_{1/3}Ta_{2/3})O_3$ Ceramics with Ultra-low Loss at Microwave Frequencies," *Proc. IEEE Int. Symp. Appl. Ferroelectric, 6th*, 118-121 (1986).
3. M. Sugiyama, T. Inuzuka and H. Kubo, "Effects of Processing on Microstructure and Dielectric Properties in $Ba(Mg_{1/3}Ta_{2/3})O_3$ Ceramics," *Ceramic Transition 15*, edited by K.M. Nair *et al.*, pp. 153-166, The American Ceramic Society Inc., Westerville, OH (1989).
4. K. Wakino and H. Tamura, "Microwave Dielectric Materials," *Ceramic Transition 8*, edited by K.M. Nair *et al.*, pp. 305-314, The American Ceramic Society Inc., Westerville, OH (1989).
5. K. Matsumoto, H. Tamura and K. Wakino, "$Ba(Mg_{1/3}Ta_{2/3})O_3$-$BaSnO_3$ High-Q Dielectric Resonator," *Jpn. J. Appl. Phys.*, **30**(8B), 2347-2349 (1991).
6. O. Renoult, J. Boilot and F. Chaput, "Sol-gel Processing and Microwave Characteristics of $Ba(Mg_{1/3}Ta_{2/3})O_3$ Dielectrics," *J. Am. Ceram. Soc.*, **75**(12), 3337-3340 (1992).
7. K. Kakegawa, T. Wakabayashi and Y. Sasaki, "Preparing of $Ba(Mg_{1/3}Ta_{2/3})O_3$ by Using Oxine," *J. Am. Ceram. Soc.*, **69**(4), C82-C83 (1986).

8. K. Tochi, "Improvement of Sinterbility of $Ba(Mg_{1/3}Ta_{2/3})O_3$ Powder Compacts by $BaTa_2O_6$ Additions," *J. Ceram. Soc. Jpn.,* **100**(12), 1464-1466 (1992).
9. F. Chaput, J. P. Boilot and A. Bauger, "Alkoxide-hydroxide Route to Synthesize $BaTiO_3$-based Powders," *J. Am. Ceram. Soc.,* **73**(4), 942-948 (1990).
10. J. A. Lee, J. J. Kim, H. Y. Lee, T. H. Kim and T. G. Choy, "Effect of Calcining Temperature on the Sintering Behaviors and Microwave Dielectric Properties of $Ba(Mg_{1/3}Ta_{2/3})O_3$ Ceramics," *J. Kor. Ceram. Soc.*, **31**(12), 1561-1569 (1994).
11. J. A. Lee, J. J. Kim, H. Y. Lee, T. H. Kim and T. G. Choy, "Effect of MgO Content on Microstructural Evoluation and Microwave Dielectric Properties of $Ba(Mg_{1/3}Ta_{2/3})O_3$ Ceramics," *J. Kor. Ceram. Soc.*, **31**(11), 1299-1306 (1994).
12. W. Jander, *Z. Anorg. Allgem. Chem.*, **163**, 1 (1927).
13. H. Schmalzried, "Chemical Kinetics of Solids," *VCH Verlagsgesellschaft mbH*, D-69451 Weinheim, F. R. Germany, pp.157 (1995).